

Application of a high-resolution in vitro human MDR1-MDCK assay and in vivo studies in preclinical species to improve prediction of CNS drug penetration

Licong Jiang | Sanjeev Kumar | Marc Nuechterlein | Marissa Reyes | Dao Tran | Clifford Cabebe | Peggy Chiang | James Reynolds | Scott Carrier | Yongkai Sun | Peter Eddershaw | Tanya Hay | Weichao Chen | Bo Feng 

Vertex Pharmaceuticals, Boston, Massachusetts, USA

Correspondence

Bo Feng, Drug Metabolism and Pharmacokinetics, Vertex Pharmaceuticals, 50 Northern Ave, Boston, MA 02210, USA.
Email: Bo_Feng@vrtx.com

Funding information

Vertex Pharmaceuticals

Abstract

P-glycoprotein (P-gp, MDR1) is expressed at the blood–brain barrier (BBB) and restricts penetration of its substrates into the central nervous system (CNS). In vitro MDR1 assays are frequently used to predict the in vivo relevance of MDR1-mediated efflux at the BBB. It has been well established that drug candidates with high MDR1 efflux ratios (ERs) display poor CNS penetration. Following a comparison of MDR1 transporter function between the MDR1-MDCKI cell line from National Institutes of Health (NIH) and our internal MDR1-MDCKII cell line, the former was found to provide better predictions of in vivo brain penetration than our in-house MDR1-MDCKII cell line. In particular, the NIH MDR1 assay has an improved sensitivity to differentiate the compounds with ERs of <3 in our internal cell line and is able to reduce the risk of false negatives. A better correlation between NIH MDR1 ERs and brain penetration in rat and non-human primate (NHP) was demonstrated. Additionally, a comparison of brain penetration time course of MDR1 substrates and an MDR1 non-substrate in NHP demonstrated that MDR1 interaction can delay the time to equilibrium of drug concentration in the brain with plasma. It is recommended to select highly permeable compounds without MDR1 interaction for rapid brain penetration to produce the maximal pharmacological effect in the CNS with a quicker onset.

KEYWORDS

CNS penetration, MDR1 assay, MDR1 efflux transporter

Abbreviations: A, apical; B, basolateral; BBB, blood–brain barrier; BCRP, breast cancer resistance protein; CNS, central nervous system; ER, efflux ratio; K_{p,uu}, partition coefficient; LC-MS/MS, liquid chromatography-tandem mass spectrometry; MDCK, Madin–Darby canine kidney; MDR1, multidrug resistance protein1; MEM, minimal essential medium; PBS, phosphate-buffered saline; P-gp, P-glycoprotein.

This is an open access article under the terms of the Creative Commons Attribution-NonCommercial License, which permits use, distribution and reproduction in any medium, provided the original work is properly cited and is not used for commercial purposes.

© 2022 The Authors. *Pharmacology Research & Perspectives* published by John Wiley & Sons Ltd, British Pharmacological Society and American Society for Pharmacology and Experimental Therapeutics.

1 | INTRODUCTION

The blood–brain barrier (BBB) is a physiological barrier formed by brain capillary endothelial cells with tight junctions,^{1,2} which restricts penetration of compounds into the brain. Brain penetration is essential for compounds with the site of action in the central nervous system (CNS), whereas for compounds that target peripheral sites, BBB penetration may need to be minimized to reduce potential CNS-related side effects. Therefore, it is critical to design and select compounds with appropriate brain penetration properties for drug targets that reside within or outside the CNS during the drug discovery phase. The kinetics of brain drug penetration consists of two aspects: the extent of drug distribution to the brain (vs. blood) at equilibrium and the time required to achieve brain distribution equilibrium. The extent of brain distribution at equilibrium is often quantified by the brain-to-plasma partitioning coefficient or concentration ratio based on either total or unbound drug concentrations at steady state (K_p and $K_{p,uu}$).^{3–5} Because only the unbound drug is expected to bind to the target^{6,7} and produce therapeutic effects, the brain-to-plasma $K_{p,uu}$ is considered more pharmacologically relevant and widely used to describe the extent of brain penetration. It is well known that brain-to-plasma $K_{p,uu}$ depends on the contribution of uptake and efflux transporters to drug transport at the BBB.⁸ If no drug transporters contribute significantly to brain penetration, free drug concentration of non-acids in the brain should theoretically be equal to the free drug concentration in plasma at steady state, and the brain-to-plasma $K_{p,uu}$ should be 1.

P-glycoprotein (P-gp, MDR1, ABCB1) is an important efflux drug transporter that is highly expressed at the BBB and functions to actively efflux compounds out of the brain, thereby limiting the extent of CNS drug penetration. The fact that very few marketed CNS drugs are substrates of human MDR1 transporter highlights its important role in CNS drug penetration.^{9,10} However, prediction of human brain penetration for substrates of MDR1 using preclinical models is challenging because of the throughput, cost, and potential species differences in transporter affinity and expression.^{11,12} Thus, it is desirable to develop a robust and high throughput human MDR1 transporter assay to rapidly deselect MDR1 substrates during CNS drug discovery and development. Literature data have suggested a good in vitro to in vivo correlation (IVIVC) with the MDR1 assay and demonstrated that in vitro MDR1 substrate assays can help quantitatively predict the extent of CNS penetration of drug candidates and guide chemistry SAR to minimize the liability of MDR1 interaction.^{10,13–15} Therefore, development of an in vitro MDR1 transporter assay with a high fidelity to characterize compound interactions with MDR1 is crucial to understand the impact of MDR1 efflux transporters on CNS penetration and help quantitatively predict CNS penetration in vivo.

Our current MDR1-MDCKII cells were developed internally previously, and the MDR1 assay had been validated with the well-established MDR1 substrates, for example, quinidine and verapamil. The current MDR1-MDCKII cells had been used to support

multiple projects, but we recently discovered that the current MDR1 assay was not able to differentiate compounds with MDR1 efflux ratios (ERs) of <3 . As a result, compounds with MDR1 ERs of <3 could have a high or a low CNS penetration in rat brain-to-plasma $K_{p,uu}$ studies. Therefore, the correlation between in vitro MDR1 assay and in vivo rat brain penetration was suboptimal. In order to develop a higher resolution in vitro MDR1 assay to support drug discovery efforts, an MDR1-MDCKI cell line from National Institutes of Health (NIH) laboratories was validated and compared with our current MDR1-MDCKII cell line. A set of internal compounds from Vertex projects with available brain penetration data in rats and non-human primates (NHPs), was identified to provide relevant in vivo context for the interpretation of the in vitro MDR1 assay. The data from the in vitro MDR1 assay were compared with brain exposure in rats and NHPs to assess the correlation between the in vitro MDR1 assay and in vivo brain penetration.

Although the extent of brain penetration or achievement of high brain $K_{p,uu}$ is the most important attribute for compounds targeting the CNS, the time to reach distribution equilibrium in the brain could be another vital property when time to onset of pharmacological action is important. Many diseases, such as acute pain,¹⁶ hypnosis,¹⁷ status epilepticus,¹⁸ and stroke,¹⁹ require compounds to have a fast CNS penetration to enable rapid onset of action. Previous studies have suggested that high passive permeability is required for a fast brain penetration.^{8,20,21} In addition to passive permeability at the BBB, it is valuable to evaluate the effect of P-gp efflux on the time to reach brain equilibrium, which could help develop strategies to select rapidly brain-penetrant compounds in CNS drug discovery.

The main goal of our studies was to evaluate the performance of in vitro human MDR1 assays so that appropriate strategies can be deployed for profiling new chemical entities with MDR1 interactions in relation to their distribution in the CNS. Additional insights were obtained regarding the impact of MDR1 efflux on the time for brain concentration to reach equilibrium with plasma concentration. The learnings can help develop strategies for discovery of optimal CNS-penetrant drugs.

2 | MATERIALS AND METHODS

2.1 | Materials

The human MDR1-transfected MDCKII cell line (MDR1-MDCKII) was generated at Vertex Pharmaceuticals, and the human MDR1-transfected MDCKI cell line (MDR1-MDCKI) was obtained from NIH Laboratory. MDR1-MDCKII and MDCKII cells were cultured in media consisting of Dulbecco's Modified Eagle's Media (low glucose), 25 mM HEPES, 10% fetal bovine serum, 1% non-essential amino acids, and 100 units/ml penicillin/streptomycin at 37°C, 5% CO₂ and 85% relative humidity. MDR1-MDCKI cells were cultured in media consisting of Dulbecco's Modified Eagle's Media (high

glucose), 10% fetal bovine serum, 5 mM L-glutamine, 80 ng/ml colchicine, and 50 units/mL penicillin/streptomycin at 37°C, 5% CO₂ and 85% relative humidity.

2.2 | Transporter transwell assays

A high-throughput, 96-well transwell assay method similar to that described previously¹⁰ was used. On day 1, MDR1-MDCKI, MDR1-MDCKII and MDCKII cells were seeded at a density of 60 000 cells/cm² onto Corning (Corning, NY) 96-well cell culture plates (1 μm pore size, 0.143 cm² growth areas). The cell monolayers were cultured at 37°C, 5% CO₂ and 85% relative humidity. The assays were performed on day 4.

Monolayer integrity, positive controls, and recovery were routinely measured to make sure that data were reportable. Lucifer Yellow A-B transport was less than 2% in every experiment to ensure monolayer integrity. The high permeability control was metoprolol and the positive control for MDR1 was quinidine. All data for controls were within the acceptable range before the data were reported. Recovery was above 70% in every experiment.

2.3 | Transwell assay procedures

All transwell assays were performed in HBSS buffer. To increase recovery of compounds with high nonspecific binding, 0.1% BSA was added to the receiver chamber. Transwell assays were performed at 1 μM concentration of compounds (≥100 μM stock solutions diluted into buffer). Transporter studies started by adding compound solutions into donor chambers and measuring appearance of compounds in receiver chambers after 90 min. Before incubation, donor samples at 0 min were collected. After 90 min of incubation, samples were collected for both donor and receiver chambers. Post-experimental incubation of lucifer yellow (100 μM, A-B transport) was carried out to confirm the integrity of the cell monolayer during incubation of test compounds.

2.4 | Transwell data analysis

The methods similar to that reported previously¹⁰ were used to determine compound apparent permeability (P_{app}) values for transwell studies. P_{app} values of the test compounds were determined using the following equation:

$$P_{app} = (dQ/dt) / (A \times C_0),$$

where dQ/dt is the rate of appearance of the test compounds in the receiver compartment, A is the surface area of the membrane (0.143 cm²), C_0 is the initial concentration (at 0 min) of test compounds in donor chamber.

The ER was calculated by the following equation:

$$\text{Efflux ratio} = (P_{app, B-A} / P_{app, A-B}).$$

2.5 | Rat brain-to-plasma K_{p,uu} experiment

All animal studies were conducted in accordance with the animal care and use procedures approved by Vertex IACUC. Male Sprague Dawley rats (Charles River Laboratories, Hollister) were allowed access to food and water ad libitum and were administered compounds via oral gavage at 3 to 30 mg/kg depending on compound clearance and oral bioavailability to achieve sufficient systemic exposure. At 1–4 h (T_{max}) post dose, blood (~0.3 ml) was collected into tubes containing K₂EDTA, centrifuged, and plasma was collected and stored at approximately –80°C prior to bioanalysis. The rats were anesthetized, and the organs were systemically perfused; brain tissues were removed, weighed, and stored at approximately –80°C prior to analysis.

2.6 | NHP brain-to-plasma and CSF-to-plasma K_{p,uu} experiment

All NHP brain and CSF K_{p,uu} studies were performed using animals already assigned for termination. Compounds were administered either individually or as a cassette of three compounds to three or four cynomolgus monkeys via oral gavage at a dose volume of 5 ml/kg. At 2–4 h (~ T_{max}) post-dose, blood was collected via a femoral vein into tubes containing K₂EDTA and then centrifuged to obtain plasma. CSF was collected from the lumbar spinal region following euthanasia. The brain was excised, rinsed with saline and blotted dry as appropriate, weighed, and frozen at approximately –80°C until analysis.

2.7 | NHP brain-to-plasma and CSF-to-plasma K_{p,uu} time course experiment

NHP brain-to-plasma K_{p,uu} studies were performed using NHPs already assigned for termination. Three compounds (antipyrene, Vertex proprietary compounds A and B) were co-formulated in 10% captisol in sterile water and were administered intravenously as a 15 min infusion via a saphenous or cephalic vein to a total of six cynomolgus monkeys. Blood, CSF, and brain were collected from 2 animals/time point at approximately 17, 30, and 60 min after the start of the infusion. Blood was taken from the vena cava into tubes containing K₂EDTA and was centrifuged to obtain plasma. The CSF and brain were collected using the similar procedure as described earlier.

2.8 | Plasma protein binding and brain tissue binding

The methods similar to that reported previously were used to measure plasma protein binding and tissue binding.²² A Rapid Equilibrium Device (RED) (Thermo Fisher Scientific) was used for free fraction

determination in plasma and tissue homogenates. On the day of the experiment, brains were homogenized with an Omni TH Handheld tissue homogenizer in PBS at a 1:3 ratio (weight:volume). 200 μ l aliquots of brain homogenates and plasma samples were loaded into RED device (donor or red side), and 350 μ l of PBS was loaded in the receiver or white side. The RED device was agitated gently on a shaking platform at 150 rpm in a CO₂ incubator (5% CO₂) for 18 h at 37°C with saturating humidity. After 18 h of incubation, 20 μ l samples from the plasma and buffer side of each RED well were added into an equal amount of the opposite blank matrix. The samples were mixed with 300 μ l of internal standard solution in acetonitrile to precipitate proteins. The samples were then vortexed and centrifuged, and the supernatants were injected for LC-MS/MS analysis.

$$\text{Calculation of the fraction unbound: } F_u = (A_{\text{free},18\text{h}}/A_{\text{total},18\text{h}})$$

$A_{\text{free},18\text{h}}$

= Peak area ratio of analyte to internal standard in dialysis buffer in receiver chamber following 18 h of incubation,

$A_{\text{total},18\text{h}}$

= Peak area ratio of analyte to internal standard in the donor chamber following 18 h of incubation.

If dilution was involved, the following formula was used for calculating fraction unbound F_u from F_u' :

$$F_u = \frac{1/D}{[1/F_u' - 1] + 1/D}$$

where D = dilution factor (e.g., 4 for brain homogenate in this study);
 F_u' = Fraction unbound in diluted matrix

2.9 | Sample analysis by LC-MS/MS

LC-MS/MS was used for the analysis of transporter study samples and determination of plasma, CSF and brain concentrations. Agilent 1200 Infinity HTS series HPLC binary pumps coupled with CTC. Analytics PAL (LEAP) autosamplers interfaced with Applied Biosystems Sciex API 4500 or 5500 QTrap mass spectrometers were used for LC-MS/MS analysis of transporter study samples. The LC separation was carried out on a Bona-Agela (Wilmington, DE) Unisol C18 reversed-phase HPLC column (2.1 \times 30 mm, 5 μ m). The mobile phase A was 10 mM ammonium acetate aqueous solution (pH 4.0), and the mobile phase B was 50:50 (v/v) acetonitrile-methanol. The eluting gradient was 0 to 99% B from 0.0 to 0.5 min at flow rate of 1.0 ml/min, 99% B from 0.5 to 0.9 min at flow rate of 1.0 ml/min, 99% B from 0.91 to 1.0 min at flow rate of 1.8 ml/min, 0% B from 1.01 to 1.08 min at flow rate of 1.8 ml/min, and 0% B from 1.09 to 1.1 min at flow rate of 1.0 ml/min. Multiple reaction monitoring MS/MS was used to measure test compounds and internal standard simultaneously.

The brain was homogenized with PBS (1:3 weight:volume) before analysis. Plasma, CSF, and brain homogenates were protein-precipitated with organic solvents, and the supernatant was analyzed by LC-MS/MS against standard curves as described below.

Compound solid was dissolved in DMSO to obtain a 1 mg/ml stock, and the spiking solutions were prepared with serial dilutions. Rat or monkey plasma calibration standards and quality control (QC) samples were prepared by adding 10 μ l of the compound spiking solutions into 390 μ l of plasma to achieve desired dynamic ranges. 20 μ l of plasma or CSF or brain homogenates were aliquoted; matrix differences were compensated with blank plasma, blank CSF or blank brain homogenates accordingly, then protein-precipitated with 480 μ l of internal standard solution containing 10.0 ng/ml of VRT-125070 in 0.1% formic acid:acetonitrile:methanol (20:40:40). The samples were thoroughly mixed before centrifugation at 12 000 rpm for 10 min to obtain supernatant for LC/MS/MS analysis. 10 μ l of the supernatant was injected using the CTC PAL autosampler. The LC system consisted of Shimadzu LC with mobile phases of 0.1% formic acid in water (A) and 0.1% formic acid in acetonitrile (B), and a Phenomenex Synergy C8 (3 μ , 30 mm \times 2 mm) column. The flow rate was 0.5 ml/min, with a generic gradient (the initial gradient starting at 10% B, and increasing in linear fashion to 90% B from 0.5 to 2 min). Multiple reaction monitoring was performed using Applied Biosystems (Foster City, CA) Sciex API 4000 or 5000 mass spectrometers for compound and internal standard measurements.

All authors consciously assure that the following are fulfilled: (1) This material is the authors' own original work, which has not been previously published elsewhere. (2) The paper is not currently being considered for publication elsewhere. (3) The paper reflects the authors' own research and analysis in a truthful and complete manner. (4) The paper properly credits the meaningful contributions of co-authors. (5) The results are appropriately placed in the context of prior and existing research. (6) All sources used are properly disclosed (correct citation). (7) All authors have been personally and actively involved in substantial work leading to the paper and will take public responsibility for its content.

3 | RESULTS

3.1 | Functional comparison between our current MDR1-MDCKII cell line and the MDR1-MDCKI cell line from NIH laboratories

Recently, we discovered that our internal MDR1-MDCKII assay did not have the resolution to differentiate compounds with MDR1 ERs of <3. As such, we have been striving to identify an improved MDR1 cell line which can better differentiate compounds with ERs of <3. A set of ~70 proprietary compounds from discovery projects with ERs of <3 in our current MDR1 assay was selected to compare the functional MDR1 activity between our existing MDR1-MDCKII cell line and an alternative MDR1-MDCKI cell line from the NIH laboratories. Figure 1 shows the comparison of ERs in two cell lines for this set of

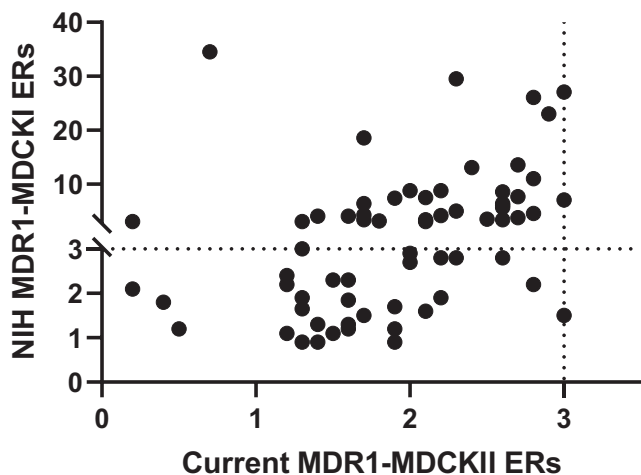


FIGURE 1 Comparison of efflux ratios (ERs) between NIH MDR1-MDCKI and our current MDR1-MDCKII for a set of compounds from discovery projects with ERs < 3. ER of 3 is used as the cutoff to classify MDR1 substrates in both NIH MDR1-MDCKI cells and our current MDR1-MDCKII cells. ER equals to $B_A \text{ Papp}$ ($n = 3$) divided by $A_B \text{ Papp}$ ($n = 3$) in different cell lines

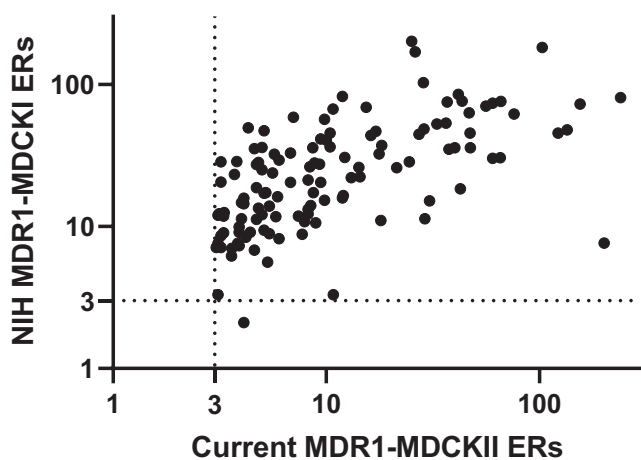


FIGURE 2 Comparison of efflux ratios between NIH MDR1-MDCKI and our current MDR1-MDCKII for a set of compounds from discovery projects with efflux ratios > 3. Efflux ratio of 3 is used as the cutoff to classify MDR1 substrates in both NIH MDR1-MDCKI cells and our current MDR1-MDCKII cells. Efflux ratio equals to $B_A \text{ Papp}$ ($n = 3$) divided by $A_B \text{ Papp}$ ($n = 3$) in different cell lines

compounds. The data in Figure 1 clearly indicated that over the ER range of 1 to 3 in our current MDR1 assay, the NIH MDR1 cell line demonstrated a substantially greater dynamic range, with ERs ranging from 1 to ~30. Interestingly, for compounds with ERs of > 3 in our existing MDR1 assay, the ERs generated from the two cell lines were aligned with each other, but ERs from NIH MDR1 were mostly higher than ERs from our current MDR1 assay (Figure 2). These data suggest that NIH MDR1 assay has higher MDR1 efflux activity, is more sensitive, and provides higher resolution for differentiating compounds with MDR1 ERs of < 3 in our current assay.

3.2 | Correlation between MDR1 assay and brain-to-plasma K_{p,uu} in rats

A set of proprietary compounds with brain-to-plasma K_{p,uu} data in rats was selected to compare the correlation with the ERs generated from our internal MDR1-MDCKII cells or the MDR1-MDCKI cells from NIH (Figure 3). Based on internal validation using the reported positive and negative controls of MDR1 substrates in literature, an ER of 3 was determined as the cutoff to classify MDR1 substrates in both internal MDR1 and the NIH MDR1 assays. Similarly, a brain-to-plasma K_{p,uu} of greater than 0.5 was identified as a cutoff to classify compounds as freely CNS penetrant versus those with impaired CNS penetration due to efflux transport. Figure 3 shows the correlation between MDR1 ERs from our internal cell line and those from the NIH cell line with brain K_{p,uu} in rats. For our internal MDR1 cell line, all compounds are in quadrants 2, 3, and 4, whereas, for NIH MDR1 cell line, all compounds are in quadrants 2 and 4 except the one compound which is in quadrant 3. The data indicate that when ERs from two cell lines were higher than the cutoff of 3, the brain K_{p,uu} values in rats were lower than 0.5. Thus, when compounds were identified as MDR1 substrates in vitro, they exhibited impaired CNS penetration in rats, as expected. Interestingly, 14 out of 21 compounds with ERs < 3 from our existing MDR1 assay exhibited brain K_{p,uu} values lower than 0.5 suggesting that some compounds classified as MDR1 non-substrates in our current in vitro MDR1 assay could have impaired brain penetration. Consequently, our current MDR1 assay could generate false negatives as efflux substrates. In contrast to our internal MDR1 cell line, NIH MDR1 ERs correlated with brain K_{p,uu} in rats much better. This was due to the fact that a fraction of the compounds with ERs of < 3 in our current MDR1 assay shifted to ERs of > 3 in the NIH MDR1 assay. Therefore, the potential false negatives generated from our internal MDR1 assay were confirmed to be positive in the NIH MDR1 assay, and this aligned with the impaired brain penetration in rats. These data indicate that the NIH MDR1 assay provides a greater differentiation and resolution to identify MDR1 substrates compared with our current MDR1 assay.

3.3 | Correlation between MDR1 efflux ratios with CSF-to-plasma K_{p,uu} and brain-to-plasma K_{p,uu} in non-human primates

Because of ethical and practical constraints, it is not feasible to acquire NHP brain K_{p,uu} data for a large set of compounds. Because CSF is considered a surrogate of unbound brain concentration, a set of 27 proprietary compounds with available CSF K_{p,uu} data in NHP was selected to compare MDR1 transporter function between our internal MDR1 cell line and the NIH MDR1 cell line (Figure 4). For compounds with ERs of < 3 or ERs of 3–5 in our internal MDR1 assay, CSF K_{p,uu} values in NHPs ranged from 0.2 to slightly higher than 1, with no apparent correlation between the two. In contrast, the NIH MDR1 assay was able to better resolve compounds, and the range of NIH MDR1 ERs for the same set of compounds was expanded

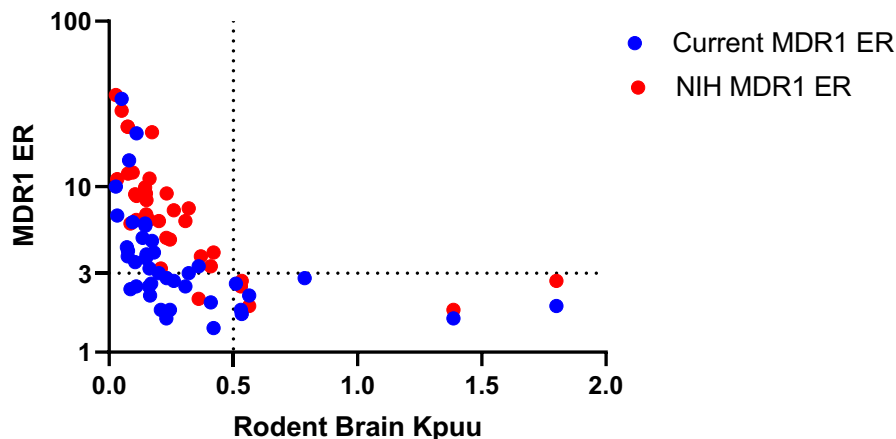


FIGURE 3 Correlation between rat brain-to-plasma $K_{p,uu}$ and efflux ratios from our current MDR1-MDCKII and NIH MDR1-MDCKI for a set of compounds from discovery projects. Brain-to-plasma $K_{p,uu}$ of 0.5 is used as a cutoff for brain penetration, and efflux ratio of 3 is used as the cutoff to classify MDR1 substrates in both NIH MDR1-MDCKI cells and the current MDR1-MDCKII cells. Efflux ratio equals to B_A Papp ($n = 3$) divided by A_B Papp ($n = 3$) in different cell lines. Quadrant 1 is upper right, quadrant 2 is upper left, quadrant 3 is lower left, and quadrant 4 is lower right

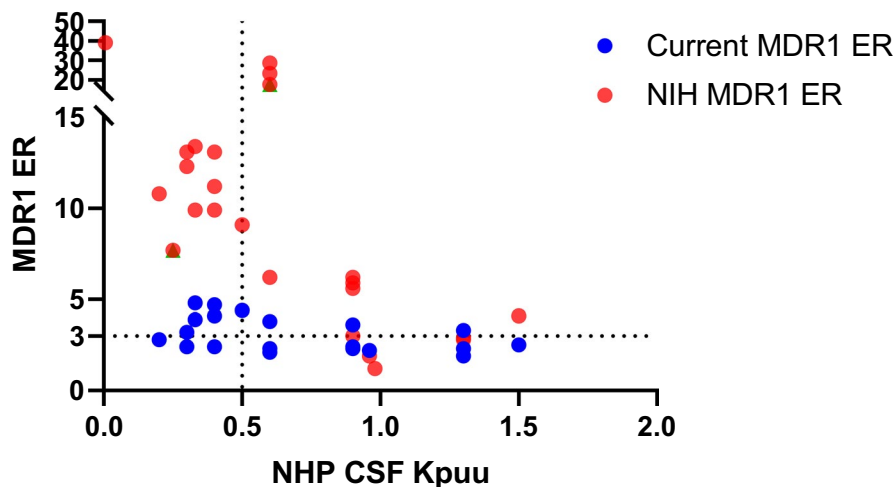


FIGURE 4 Correlation between non-human primate CSF-to-plasma $K_{p,uu}$ and efflux ratios from our current MDR1-MDCKII and NIH MDR1-MDCKI for a set of compounds from discovery projects. CSF-to-plasma $K_{p,uu}$ of 0.5 is used as a cutoff for brain penetration, and efflux ratio of 3 is used as the cutoff to classify MDR1 substrates in both NIH MDR1-MDCKI cells and the current MDR1-MDCKII cells. Efflux ratio equals to B_A Papp ($n = 3$) divided by A_B Papp ($n = 3$) in different cell lines

from 1 to nearly 40, and displayed an inverse correlation with CSF $K_{p,uu}$ in NHP. None of the compounds with ERs of <3 in the NIH MDR1 assay exhibited any appreciable impairment of CNS penetration based on CSF $K_{p,uu}$ in NHP, whereas compounds with impaired CNS penetration (NHP CSF $K_{p,uu} < 0.5$) had NIH MDR1 ERs of >3 .

Certainly, it is more valuable to establish a correlation between MDR1 ERs with brain-to-plasma $K_{p,uu}$ in NHPs. Although more limited in scope, we obtained NHP brain $K_{p,uu}$ values for a subset of 10 compounds (9 proprietary compounds and antipyrine) (Table 1), which showed a good correlation with NIH MDR1 ERs (Figure 5). Compounds with NIH MDR1 ERs of <3 exhibited an NHP brain $K_{p,uu}$ of near unity, whereas those with NIH MDR1 ERs of >3 showed an inverse correlation of brain $K_{p,uu}$ with increasing ER.

Additionally, it is of interest to understand the potential species difference in CNS penetration between rat and NHP. Hence, the brain penetration of this set of compounds, including seven MDR1 substrates and three non-MDR1 substrates, in NHPs was compared with rats (Figure 6). As expected, both rat and NHP

brain $K_{p,uu}$ of the three non-MDR1 substrates were close to 1, except that rat brain $K_{p,uu}$ of compound 8, a non-MDR1 substrate, was dramatically lower than 1, and the reason remains to be answered. The data demonstrated that NHP brain $K_{p,uu}$ values increased notably relative to rat brain $K_{p,uu}$ for all MDR1 substrates, except for compounds 1, 5 and 7. Subsequently, it was confirmed that compound 1 is a BCRP and MDR1 dual substrate, and compounds 5 and 7 have NIH MDR1 ERs of >100 with a very low brain $K_{p,uu}$ (<0.05).

3.4 | Comparison of csf and unbound brain concentrations for MDR1 substrates in non-human primates

To investigate the utility of CSF concentration as a surrogate for unbound brain concentration in NHP, CSF and unbound brain concentrations of the same 10 compounds were measured (Table 1).

TABLE 1 Non-human primate (NHP) and rat brain-to-plasma K_{puu}, NHP CSF-to-plasma K_{puu}, human NIH MDR1 and breast cancer resistance protein (BCRP) efflux ratio, passive permeability and NHP plasma protein and brain binding of nine proprietary compounds and antipyrine

Compound#	NHP K _{p,uu} brain	NHP K _{p,uu} CSF	MDR1 efflux ratio (ER ^a)	BCRP ER ^a	MDCK A-B Papp (×10 ⁻⁶ cm/s)	Fu,plasma	Fu,brain	Rat K _{p,uu} brain
1	0.16 (0.15, 0.17)	0.33 (0.28, 0.39)	9.9	14.9	11.4 ± 1.8	0.030	0.006	0.12 ± 0.03
2	0.41 (0.36, 0.46)	0.42 (0.38, 0.46)	13.1	2.8	12.5 ± 3.4	0.13	0.019	0.26 ± 0.01
3	0.29 ± 0.05	0.43 ± 0.07	12.1	3.9	8.2 ± 3.2	0.055	0.014	0.16 ± 0.02
4	0.27 ± 0.03	0.67 ± 0.10	13.4	1.6	9.9 ± 0.3	0.007	0.005	0.09 ± 0.03
5	0.026 ± 0.010	<0.020 ^b	172.0	21.0	0.7 ± 0.4	0.022	0.029	0.005 ± 0.002
6	0.13 ± 0.00	>1 ^d	14.1	1.3	5.8 ± 1.8	0.003	0.003	0.04 ± 0.01
7	<0.004	0.026 ± 0.016	116.0	39.8	0.4 ± 0.3	0.009	0.009	0.01 ± 0.00
8	1.24 ± 0.24	0.86 ± 0.19	2.8	3.0	5.0 ± 1.3	0.006	0.003	0.21 ± 0.03
9	1.28 ± 0.21	0.69 ± 0.07	1.9	2.3	6.2 ± 0.5	0.014	0.005	0.57 ± 0.09
Antipyrine	0.96 (0.91, 1.01)	1.00 (0.92, 1.08)	1.0	0.9	32.8 ± 9.0	0.95	1.0 ^c	1.0 ^e

Note: Data are presented as mean ± SD from three replicates except where data from only two replicates were available, in which cases means along with individual data (in parentheses) are listed.

^aER equals to B_A Papp (n = 3) divided by A_B Papp (n = 3) in different cell lines.

^bValue was averaged from 0.0255, <0.0183, <0.0148, but two of the values were below LLOQ (lower limit of quantitation).

^cAntipyrine fu,brain is assumed to be 1.00, since in brain tissue homogenate (1:3 tissue:PBS), antipyrine fu was ~1.

^dCompound 6 CSF values (n = 3) were all >1 with some variabilities.

^eAntipyrine rat brain K_{puu} was calculated based on the data in Nagaya et al. (2016).²⁹

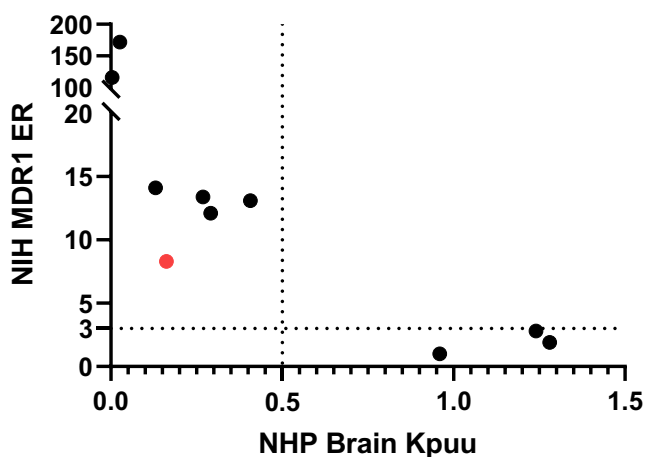


FIGURE 5 Correlation between non-human primate (NHP) brain-to-plasma K_{p,uu} and efflux ratios from NIH MDR1-MDCKI of 9 proprietary compounds and antipyrine. Brain-to-plasma K_{p,uu} of 0.5 is used as a cutoff for brain penetration. The NHP brain-to-plasma K_{p,uu} and efflux ratios values can be found in Table 1

Figure 7 shows the brain-to-plasma K_{p,uu} and CSF-to-plasma K_{p,uu} values of the 7 MDR1 substrates, which were appreciably lower than unity with exception of compound 6 CSF K_{puu} ~1. In contrast, brain K_{p,uu} and CSF K_{p,uu} values of the three non-MDR1 substrates were close to 1. Although the CSF K_{p,uu} showed a trend of overestimating brain K_{p,uu} of MDR1 substrates, the CSF K_{p,uu} were generally in a good agreement with brain K_{p,uu} (within 3-fold) except for two

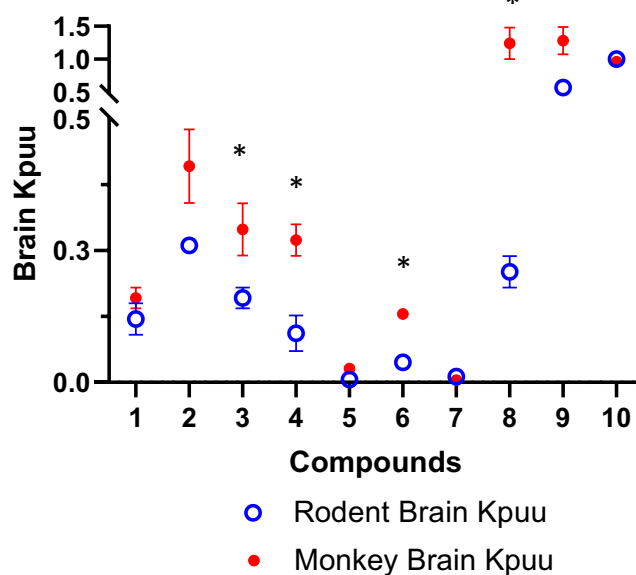


FIGURE 6 Comparison of brain-to-plasma K_{p,uu} between rat and NHP of the same 10 compounds including 7 MDR1 substrates and 3 non-MDR1 substrates. Data points represent mean ± SD. **p* < .01, brain-to-plasma K_{p,uu} in rat versus NHP

MDR1 substrates, compounds 6 and 7, which had very high protein binding with fu,_p < 0.01 and very low brain K_{p,uu}. These data further support the use of CSF drug concentration as a surrogate for unbound brain drug concentration.

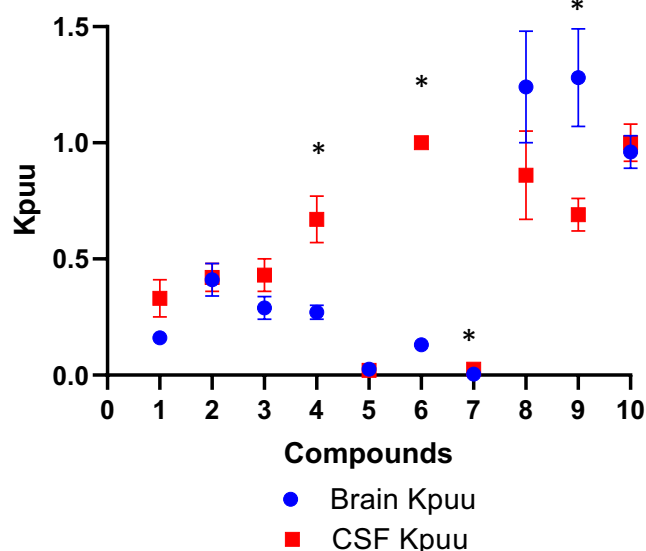


FIGURE 7 Comparison of brain-to-plasma $K_{p,uu}$ with CSF-to-plasma $K_{p,uu}$ of the same 10 compounds including 7 MDR1 substrates and 3 non-MDR1 substrates in non-human primates. Data points represent mean \pm SD. * $p < .01$, brain-to-plasma $K_{p,uu}$ versus CSF-to-plasma $K_{p,uu}$

3.5 | Comparison of CSF-to-plasma $K_{p,uu}$ and brain-to-plasma $K_{p,uu}$ time courses in non-human primates

Another question of interest is whether MDR1 could influence the rate of drug penetration into the CNS. Three compounds, including antipyrine, and proprietary compounds 1 and 2 were selected to explore how MDR1 might impact the kinetics of drug distribution into the CNS in NHP. The MDR1/BCRP interactions, in vitro passive permeability, and plasma protein and brain binding of the three compounds are summarized in Table 1. Antipyrine has a high passive permeability, low plasma protein and brain tissue binding, and no MDR1/BCRP efflux transporter interactions. In contrast, compound 1 and 2 have high in vitro passive permeability, moderate-to-high plasma protein binding and high brain binding, and are MDR1 substrates with NIH MDR1 ERs of ~ 10 (Table 1). It is worth noting that compound 1 is an MDR1 and BCRP dual substrate, but compound 2 is an MDR1 only substrate. The brain and CSF $K_{p,uu}$ were measured at 0.25, 0.5, and 1 h after IV infusion at 0.5–3 mg/kg for 15 min in NHP, and Figure 8 displays the time course of brain and CSF $K_{p,uu}$ of the three compounds. For antipyrine, the unbound brain concentration reached equilibrium with unbound plasma concentration (brain $K_{p,uu}$ of ~ 1) within 15 min. However, lumbar CSF concentration of antipyrine took longer to equilibrate with plasma concentration with CSF $K_{p,uu}$ reaching unity at ~ 1 h. In contrast, both brain and CSF $K_{p,uu}$ of compounds 1 and 2 continued to increase until the final 1 h sampling time in this study. Brain and CSF $K_{p,uu}$ of compound 1 were 0.16 and 0.33 at 1 h, respectively, and both brain and CSF $K_{p,uu}$ of compound 2 were ~ 0.4 at 1 h. Because the brain $K_{p,uu}$ of compound 1 at 1 h in this study was similar to its brain $K_{p,uu}$

at 24 h following the last dose in 7-day NHP study (0.16 ± 0.03), it is reasonable to conclude that brain concentrations of compound 1 and 2 have approached equilibrium with plasma concentration at 1 h in this study as well. These data demonstrate that unlike antipyrine, brain concentrations of both compound 1 and compound 2 exhibit a delay to equilibrate with plasma. However, it took ~ 1 h for lumbar CSF to reach equilibrium with plasma for all three compounds, which is consistent with flow-limited mixing of CSF in different regions. The data further support the notion that CSF drug concentration could be a surrogate for unbound brain drug concentration with a comparable or a severalfold higher value.

4 | DISCUSSION

Because MDR1 is the major efflux transporter expressed at the BBB impacting brain penetration, it is an essential optimization parameter for the design of compounds requiring CNS penetration for efficacy, or for those that need to be restricted from accessing the CNS from a safety perspective. This has been reinforced by the fact that most CNS-penetrant drugs are not MDR1 substrates, which corroborates the importance of early assessment of MDR1 substrates in drug discovery.^{9,10} Therefore, development of a robust and reliable MDR1 transporter assay which best correlates with in vivo brain penetration to guide SAR during lead optimization is critical. At Vertex, an MDR1 assay using an MDR1-MDCKII cell line developed internally has been used to assess CNS penetration of compounds. Previous evaluation focusing on IVIVC of MDR1 ERs and rat brain penetration suggested a strong correlation between an in vitro MDR1 ER of >3 and impaired CNS penetration in rats. However, compounds with an in vitro MDR1 ER of <3 displayed a range of brain penetration properties in rats and led to potential false negatives. Thus, the current in vitro MDR1 assay did not appear to have enough resolution to differentiate compounds with ERs of <3 , and project teams had to rely on rat brain-to-plasma $K_{p,uu}$ values to differentiate compounds with ERs of <3 . In addition to the increased need for animal studies, in vivo rat brain $K_{p,uu}$ studies are relatively slow, resource intensive and have low throughput, which can lead to significantly prolonged project cycle times to select compounds with good CNS penetration. More importantly, projects targeting desirable CNS penetration prioritize compounds with MDR1 ER of <3 , which are predicted to be non-MDR1 substrates. Moreover, potential species difference in MDR1 transport could further confound the prediction of CNS penetration in human. Hence, we have been striving to develop an MDR1 assay with a high fidelity to reliably differentiate compounds with MDR1 ERs of <3 in our current MDR1 assay.

It has been reported that the MDR1-MDCKI cell line from the NIH laboratory is a better alternative MDR1 cell line which does not generate false negatives and has a stronger correlation with rodent brain penetration.^{23,24} In our extensive validation, NIH MDR1-MDCKI cells were able to better differentiate compounds that had ERs of <3 in our existing MDR1-MDCKII assay (Figure 1), demonstrating a much higher resolution for these compounds. It has been

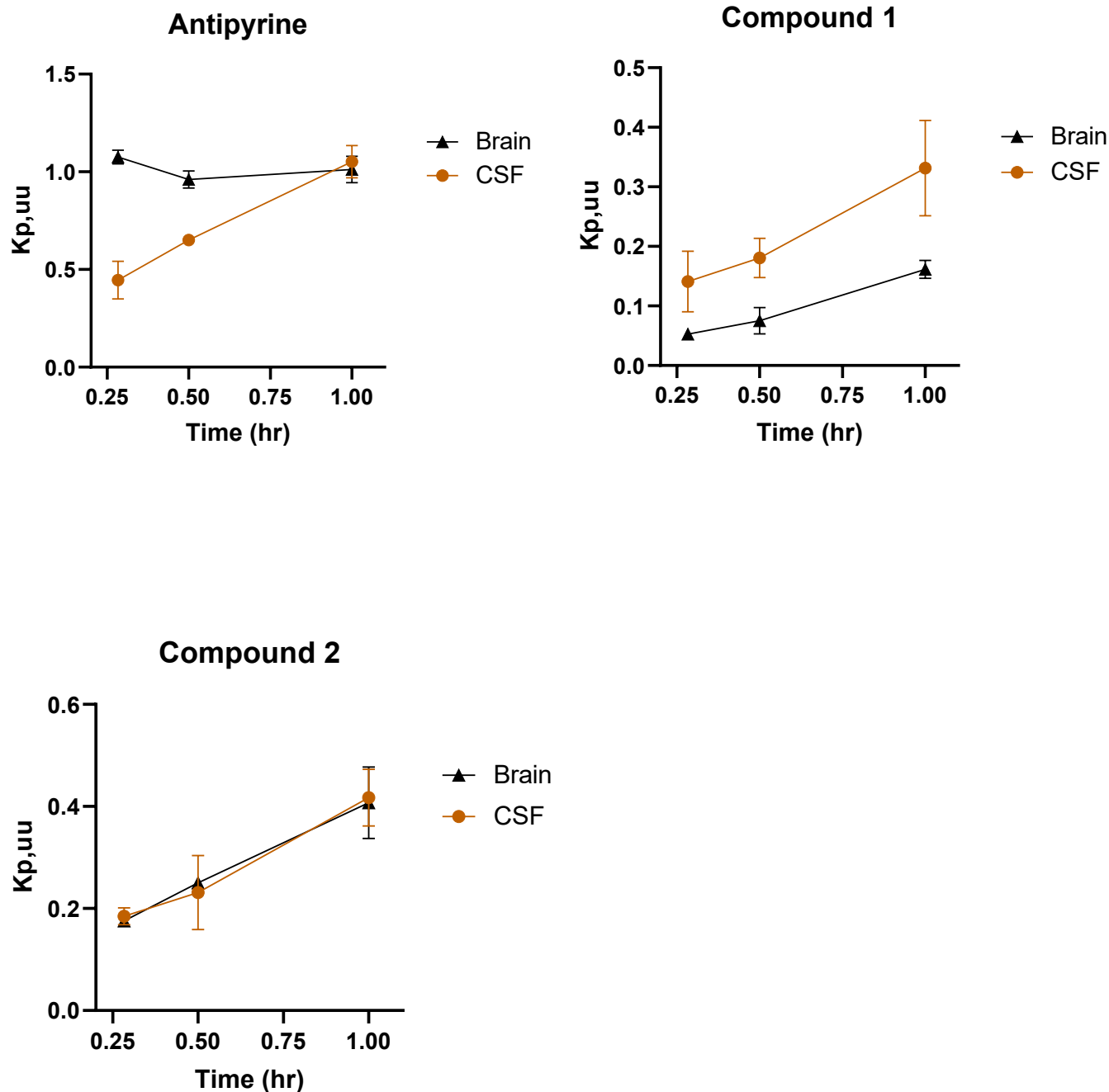


FIGURE 8 Brain-to-plasma $K_{p,uu}$ and CSF-to-plasma $K_{p,uu}$ time course for antipyrine, compounds 1 and 2 in non-human primates. Data points represent mean \pm SD from three animals

reported that NIH MDR1-MDCKI cells have ~10-fold higher expression of P-gp (29.8 pmol/mg),²³ compared with our existing MDR1-MDCKII cells (2.92 pmol/mg, internal data). Additionally, the ERs in NIH MDR1 assay are more than 10-fold higher than those in our current MDR1 assay for the well characterized MDR1 substrates, for example, quinidine and verapamil. Higher MDR1 expression and function likely contribute to a greater assay sensitivity and a larger transport dynamic range. More importantly, the NIH MDR1 assay correlated with rat brain $K_{p,uu}$ much better than our current MDR1 assay, especially in the low ER range (Figure 3). As discussed earlier, an MDR1 ER of 3 was identified as a cutoff for identifying

MDR1 substrates in vitro, whereas a brain $K_{p,uu}$ of 0.5 was used to classify compounds as having brain penetration impairment ($K_{p,uu} < 0.5$) versus being freely brain penetrant. Both our current MDR1 and NIH MDR1 assays demonstrated good alignment with rat brain penetration impairment when ERs were >3 , but our current MDR1 assay had poor correlation with rat brain distribution when ERs were <3 . Although it is possible that the in vitro and in vivo disconnect for compounds with MDR1 ERs of <3 in our current assay could potentially be due to efflux transporters other than MDR1, studies of a subset of these compounds in *Mdr1a/1b* knock out rats indicated that the brain penetration impairment in rats was due to

Mdr1 (internal data). Additionally, it has been reported that since the amino acid homology between human MDR1 and rat Mdr1a is high, the species difference in terms of substrate specificity is likely to be minimal.¹⁰ Therefore, our internal MDR1 assay could generate potential false negatives compared with rat brain penetration. On the contrary, the NIH MDR1 assay demonstrated a good correlation with rat brain K_{p,uu} for compounds with ERs of <3 with the majority of compounds with NIH ERs of <3 displayed a good brain penetration in rats (Figure 3). However, one compound marked in red did show brain penetration impairment even with NIH MDR1 ER of <3 (Figure 3). As previously mentioned, this apparent discrepancy could be due to other efflux transporters beyond MDR1 and/or species difference between human MDR1 and rat Mdr1. Thus, further studies are warranted to investigate this disagreement.

Because NHP MDR1 has the highest amino acid sequence homology with human MDR1 and the MDR1 expression levels at the BBB in NHP are more comparable with human than rat,^{11,12} it is of high interest to develop a correlation between *in vitro* human MDR1 ERs and brain penetration in NHP. This correlation, if proven, could help provide more confidence in the use of MDR1 ERs to predict CNS penetration in human. It has been reported that CSF could be a good surrogate of unbound brain concentration of MDR1 substrates in NHP.^{25,26} Because CSF K_{p,uu} is a more readily accessible parameter it is beneficial to develop the correlation between MDR1 ERs and NHP CSF K_{p,uu}. A set of compounds with available NHP CSF K_{p,uu} data was identified, and the correlation between MDR1 ERs and NHP CSF K_{p,uu} was assessed (Figure 4). There was no apparent correlation between our existing MDR1 ERs and NHP CSF K_{p,uu} data such that for MDR1 ERs of <3, NHP CSF K_{p,uu} ranged from ~0.2 to ~1. However, a better correlation between NIH MDR1 ERs and NHP CSF K_{p,uu} was observed. When NIH MDR1 ERs were <3, NHP CSF K_{p,uu} values were ~1, whereas NHP CSF K_{p,uu} for slightly more than half of compounds (11 out of 19 compounds) were lower than 0.5 when NIH MDR1 ERs were >3. It has been recognized that while CSF concentration is generally a reasonable surrogate for unbound brain concentration, CSF levels could exceed unbound brain concentration for MDR1 substrates.^{25,26} Consequently, for MDR1 substrates, when CSF K_{p,uu} is ~1, brain K_{p,uu} could be lower than 1. In contrast, for non-MDR1 substrates, when CSF K_{p,uu} is ~1, brain K_{p,uu} is likely to be ~1 as well. As such, it is not surprising that in the current study, CSF K_{p,uu} was around 1 for a few compounds with NIH MDR1 ERs of >3. On the other hand, when NHP CSF K_{p,uu} was <0.5, all NIH MDR1 ERs were >3, suggesting a good IVIVC. These data demonstrate that there is a reasonable correlation between NIH MDR1 ERs and NHP CSF K_{p,uu}, and NIH MDR1 assay can improve the prediction of CNS penetration in NHP compared with our current assay.

Ultimately, it is desirable to develop a robust correlation between human MDR1 ERs and NHP brain K_{p,uu}. However, due to the obvious ethical and practical limitations with generating NHP data, only 10 compounds (Table 1), including 9 proprietary compounds and antipyrine, with NHP brain K_{p,uu} data were available. Nonetheless, a clear correlation between NIH MDR1 ER and NHP brain K_{p,uu} was observed for these 10 compounds (Figure 5). When NIH MDR1 ERs

were <3, NHP brain K_{p,uu} was ~1, whereas when NIH MDR1 ERs were >3, NHP brain K_{p,uu} was inversely correlated with the magnitude of the ER. However, compound 1 (marked in red in Figure 5) appeared to be an outlier but it was later confirmed that compound 1 was also a substrate of breast cancer resistance protein (BCRP), another major efflux transporter expressed at the BBB. It has been reported that the brain penetration of MDR1 and BCRP dual substrates is worse than that of MDR1-specific substrates.²⁷ Our data further substantiate the NIH MDR1 assay as more predictive of brain penetration in NHP. Since NHP MDR1 and human MDR1 are highly similar in terms of transport function and expression level at the BBB,¹¹ it is expected that the NIH MDR1 assay will give a good prediction of CNS penetration in human as well.

With the data indicating the superiority of the NIH MDR1 cell line and demonstrating a good correlation of the NIH MDR1 assay with rat and NHP brain penetration, we wanted to explore the relationship of brain penetration between rat and NHP, a higher-order species, for MDR1 substrates. Based on the higher P-gp expression in rats reported in the literature,^{11,12} one would expect to see an improvement in brain exposure going from rat to NHP. A rat to NHP pair-wise analysis of brain K_{p,uu} of the same 10 compounds (Table 1), including 7 MDR1 and 3 non-MDR1 substrates, clearly indicate that this is true in majority of the cases (Figure 6). Compounds that were MDR1 substrates showed moderate improvement in brain exposure in NHP relative to rat. Interestingly, comparable brain K_{p,uu} values in rats and NHP were observed for compounds 1, 5, and 7. It was discovered later that compound 1 is a dual MDR1 and BCRP substrate. It has been reported that NHP BBB has lower expression of MDR1 and higher expression of BCRP compared with rat,^{11,12} which may have contributed to the brain K_{p,uu} of compound 1 being comparable in rat and NHP. Additionally, compound 5 and compound 7 are strong MDR1 substrates with ERs of >100, resulting in very low brain K_{p,uu} of <0.05. Because of such a low K_{p,uu}, it is likely difficult to detect an improvement in brain K_{p,uu} from rats to NHP. Overall, this comparison supports the view that brain penetration in NHP will likely be greater than rat for weak and moderate MDR1 substrates.

Additionally, we investigated the utility of CSF concentration as a surrogate of unbound brain concentration in NHP. CSF and unbound brain concentrations of the same 10 compounds were measured in NHP (Table 1). For the non-MDR1 substrates, CSF and unbound brain concentrations were similar and close to unity as expected, whereas brain K_{p,uu} values were considerably lower than 1 for MDR1 substrates (Figure 7). Moreover, the brain K_{p,uu} decreased as the MDR1 ERs increased, which is aligned with MDR1-mediated efflux at BBB being the major determinant of brain K_{p,uu} in NHP. Also consistent with the previous reports,^{25,26} CSF K_{p,uu} showed a tendency to overestimate (within threefold) brain K_{p,uu} for all, with the exception of two MDR1 substrates. Because CSF concentration is impacted by unbound brain concentration diffused through the ependymal layer between the brain and CSF, as well as unbound plasma concentration passing through the choroid plexus, it is reasonable to expect that CSF concentration could be severalfold higher than unbound brain concentration

for MDR1 substrates. Of interest, the two compounds (compound 6 and 7 in Table 1) with CSF concentration dramatically higher (> threefold) than unbound brain concentration displayed high plasma protein binding ($F_{u,p} < 0.01$) and brain binding ($F_{u,brain} < 0.01$). One possible reason for this is that the high brain binding is likely to result in a slower diffusion rate from brain to CSF; thus, the CSF concentrations could be impacted more by the unbound plasma concentrations, leading to a much greater over estimation of unbound brain concentrations. However, the exact mechanism remains to be elucidated. Based on our data, CSF concentrations can be approximated to unbound brain concentrations within threefold in NHPs.

For some CNS disorders, it is often desirable to identify compounds that can rapidly penetrate into the brain to deliver a fast onset of action and produce maximal pharmacological effect shortly after administration. Thus, the time taken for brain concentration to reach equilibrium with plasma concentration ideally needs to be as short as possible. Previous studies reported that, for most drugs, the rate of penetration into the brain is limited by perfusion of the drug across BBB. The pioneering work by Brodie et al concluded that the equilibration of drug in the CSF with that in plasma is often permeability rate limited,²⁸ and later more studies have supported that passive permeability can impact the time required for compounds to reach equilibrium between brain and plasma. Antipyrine has a high passive permeability without MDR1 transport interaction. As expected, antipyrine brain $K_{p,uu}$ reached ~1 within 15 min after dosing (Figure 8). However, it took ~1 h for lumbar CSF to equilibrate with plasma, which is consistent with this being a CSF bulk-flow-limited process. Because it is not feasible to measure unbound brain concentration in human, CSF concentration is often used as a surrogate for the unbound brain concentration. It should be emphasized that the apparent delay seen for lumbar CSF to equilibrate with plasma due to bulk flow process may not reflect a delay in brain unbound concentration equilibration for compounds with a high passive permeability and no efflux transport. Similar to antipyrine, the passive permeability of both Vertex proprietary compounds 1 and 2 were high (Table 1), but in contrast to antipyrine, the brain $K_{p,uu}$ for both compounds was lower than 1 (Figure 8), which is consistent with these being MDR1 substrates. The extent of brain $K_{p,uu}$ at equilibrium is dependent on the interactions of drug with efflux transporters, independent of the magnitude of its passive permeability. Although NIH MDR1 ERs for compounds 1 and 2 were similar, given that compound 1 was an MDR1 and BCRP dual substrate, whereas compound 2 was an MDR1 substrate only, it is not surprising that compound 1 brain $K_{p,uu}$ was slightly lower than that of compound 2. Because NHP brain $K_{p,uu}$ for compound 1 at steady state after multiple dosing was comparable with brain $K_{p,uu}$ at 1 h, it was inferred that NHP brain concentrations for both compound 1 and 2 approached or approximated equilibrium with plasma concentration at ~1 h. These data suggest that MDR1 interaction could delay the time for brain concentration to achieve equilibrium with plasma concentration. As such, transport properties could have a profound influence on the equilibrium concentration and

the time to attain equilibration of drugs in the brain, and thereby on their pharmacological effects. Another potential factor that can impact the time for brain concentration to reach the equilibrium with plasma concentration is the plasma protein or brain tissue binding. It has been reported that high brain tissue binding could prolong the time for compounds to reach equilibrium in the brain.²¹ Since both compounds 1 and 2 have moderate-to-high plasma protein and high brain tissue binding, it is difficult to conclude whether plasma protein or brain tissue binding played a significant role in the time taken for these compounds to achieve equilibrium between the brain and plasma. Further studies using MDR1 substrates with low protein binding will be helpful to further confirm the role of MDR1 interaction in the delayed distribution into the brain.

In conclusion, the present studies demonstrate the value of increased resolution and fidelity of an in vitro MDR1 assay and judicious use of in vivo studies in preclinical species for a more accurate optimization and reliable prediction of CNS drug penetration during drug discovery. In addition, our data suggest that MDR1 interaction can influence the time for drug concentrations in the brain to reach equilibrium with plasma. Consequently, compounds with high passive permeability and without MDR1 interaction are desired when rapid brain penetration and onset of pharmacological activity are required.

ACKNOWLEDGEMENTS

The work was supported by Vertex Pharmaceuticals.

DISCLOSURE

All authors declare no competing interest.

AUTHOR CONTRIBUTIONS

Participated in research design: Jiang, Kumar, Eddershaw, Hay, Chen, and Feng. Conducted experiments: Nuechterlein, Reyes, Tran, Cabebe, Chiang, Reynolds, Carrier, and Sun. Contributed new reagents or analytic tools: Nuechterlein, Reyes, Tran, Cabebe, Chiang, and Reynolds. Performed data analysis: Jiang, Sun, and Feng. Wrote or contributed to the writing of the manuscript: Jiang, Kumar, Eddershaw, Hay, and Feng.

DATA AVAILABILITY STATEMENT

All data are available in Vertex-archived notebooks.

ORCID

Bo Feng  <https://orcid.org/0000-0001-6655-766X>

REFERENCES

1. Abbott NJ, Patabendige AA, Dolman DE, Yusof SR, Begley DJ. Structure and function of the blood-brain barrier. *Neurobiol Dis.* 2010;37:13-25.
2. Rubin LL, Staddon JM. The cell biology of the blood-brain barrier. *Annu Rev Neurosci.* 1999;22:11-28.
3. Freeman BB 3rd, Yang L, Rankovic Z. Practical approaches to evaluating and optimizing brain exposure in early drug discovery. *Eur J Med Chem.* 2019;182:111643.

4. Hammarlund-Udenaes M, Bredberg U, Fridén M. Methodologies to assess brain drug delivery in lead optimization. *Curr Top Med Chem*. 2009;9:148-162.
5. Reichel A. Addressing central nervous system (CNS) penetration in drug discovery: basics and implications of the evolving new concept. *Chem Biodivers*. 2009;6:2030-2049.
6. Bouw MR, Gårdmark M, Hammarlund-Udenaes M. Pharmacokinetic-pharmacodynamic modelling of morphine transport across the blood-brain barrier as a cause of the antinociceptive effect delay in rats—a microdialysis study. *Pharm Res*. 2000;17:1220-1227.
7. Stain-Textier F, Boschi G, Sandouk P, Scherrmann JM. Elevated concentrations of morphine 6- β -D-glucuronide in brain extracellular fluid despite low blood-brain barrier permeability. *Br J Pharmacol*. 1999;128:917-924.
8. Hammarlund-Udenaes M, Paalzow LK, de Lange EC. Drug equilibration across the blood-brain barrier—pharmacokinetic considerations based on the microdialysis method. *Pharm Res*. 1997;14:128-134.
9. Doran A, Obach RS, Smith BJ, et al. The impact of P-glycoprotein on the disposition of drugs targeted for indications of the central nervous system: evaluation using the MDR1A/1B knockout mouse model. *Drug Metab Dispos*. 2005;33:165-174.
10. Feng B, Mills JB, Davidson RE, et al. In vitro P-glycoprotein assays to predict the in vivo interactions of P-glycoprotein with drugs in the central nervous system. *Drug Metab Dispos*. 2008;36:268-275.
11. Ito K, Uchida Y, Ohtsuki S, et al. Quantitative membrane protein expression at the blood-brain barrier of adult and younger cynomolgus monkeys. *J Pharm Sci*. 2011;100:3939-3950.
12. Uchida Y, Ohtsuki S, Katsukura Y, et al. Quantitative targeted absolute proteomics of human blood-brain barrier transporters and receptors. *J Neurochem*. 2011;117:333-345.
13. Chen C, Liu X, Smith BJ. Utility of Mdr1-gene deficient mice in assessing the impact of P-glycoprotein on pharmacokinetics and pharmacodynamics in drug discovery and development. *Curr Drug Metab*. 2003;4:272-291.
14. Lin JH, Yamazaki M. Clinical relevance of P-glycoprotein in drug therapy. *Drug Metab Rev*. 2003;35:417-454.
15. Polli JW, Wring SA, Humphreys JE, et al. Rational use of in vitro P-glycoprotein assays in drug discovery. *J Pharmacol Exp Ther*. 2001;299:620-628.
16. Jung YS, Kim DK, Kim MK, Kim HJ, Cha IH, Lee EW. Onset of analgesia and analgesic efficacy of tramadol/acetaminophen and codeine/acetaminophen/ibuprofen in acute postoperative pain: a single-center, single-dose, randomized, active-controlled, parallel-group study in a dental surgery pain model. *Clin Ther*. 2004;26:1037-1045.
17. Hardman JG, Limbird LE, Gilman AG. *Goodman & Gilman's The Pharmacological Basis of Therapeutics*, 10th ed. McGraw-Hill; 2001.
18. Li L, Gorukanti S, Choi YM, Kim KH. Rapid-onset intranasal delivery of anticonvulsants: pharmacokinetic and pharmacodynamic evaluation in rabbits. *Int J Pharm*. 2000;199:65-76.
19. Adams HP Jr, Leira EC. Treatment of acute ischemic stroke. *Drugs Today*. 1998;34:655-660.
20. Di L, Kerns EH, Fan K, McConnell OJ, Carter GT. High throughput artificial membrane permeability assay for blood-brain barrier. *Eur J Med Chem*. 2003;38:223-232.
21. Liu X, Smith BJ, Chen C, et al. Use of a physiologically based pharmacokinetic model to study the time to reach brain equilibrium: an experimental analysis of the role of blood-brain barrier permeability, plasma protein binding, and brain tissue binding. *J Pharmacol Exp Ther*. 2005;313:1254-1262.
22. Feng B, Pemberton R, Dworakowski W, et al. Evaluation of the utility of PXB chimeric mice for predicting human liver partitioning of hepatic organic anion-transporting polypeptide transporter substrates. *Drug Metab Dispos*. 2021;49:254-264.
23. Feng B, West M, Patel NC, et al. Validation of human MDR1-MDCK and BCRP-MDCK cell lines to improve the prediction of brain penetration. *J Pharm Sci*. 2019;108:2476-2483.
24. Kikuchi R, de Morais SM, Kalvass JC. In vitro P-glycoprotein efflux ratio can predict the in vivo brain penetration regardless of biopharmaceutics drug disposition classification system class. *Drug Metab Dispos*. 2013;41:2012-2017.
25. Nagaya Y, Katayama K, Kusuha H, Nozaki Y. Impact of P-glycoprotein-mediated active efflux on drug distribution into lumbar cerebrospinal fluid in nonhuman primates. *Drug Metab Dispos*. 2020;48:1183-1190.
26. Nagaya Y, Nozaki Y, Kobayashi K, et al. Utility of cerebrospinal fluid drug concentration as a surrogate for unbound brain concentration in nonhuman primates. *Drug Metab Pharmacokinet*. 2014;29:419-426.
27. Zhou L, Schmidt K, Nelson FR, Zelesky V, Troutman MD, Feng B. The effect of breast cancer resistance protein and P-glycoprotein on the brain penetration of flavopiridol, imatinib mesylate (Gleevec), prazosin, and 2-methoxy-3-(4-(2-(5-methyl-2-phenyloxazol-4-yl)ethoxy)phenyl)propanoic acid (PF-407288) in mice. *Drug Metab Dispos*. 2009;37:946-955.
28. Brodie BB, Kurz H, Schanker LS. The importance of dissociation constant and lipid-solubility in influencing the passage of drugs into the cerebrospinal fluid. *J Pharmacol Exp Ther*. 1960;130:20-25.
29. Nagaya Y, Nozaki Y, Takenaka O, et al. Investigation of utility of cerebrospinal fluid drug concentration as a surrogate for interstitial fluid concentration using microdialysis coupled with cisternal cerebrospinal fluid sampling in wild-type and Mdr1a(-/-) rats. *Drug Metab Pharmacokinet*. 2016;31:57-66.

How to cite this article: Jiang L, Kumar S, Nuechterlein M, et al. Application of a high-resolution in vitro human MDR1-MDCK assay and in vivo studies in preclinical species to improve prediction of CNS drug penetration. *Pharmacol Res Perspect*. 2022;10:e00932. doi:[10.1002/prp2.932](https://doi.org/10.1002/prp2.932)